Marine Ecology. ISSN 0173-9565

ORIGINAL ARTICLE

Age and growth in olive ridley seaturtles (*Lepidochelys olivacea*) from the North-central Pacific: a skeletochronological analysis

George R. Zug[1], Milani Chaloupka[2] & George H. Balazs[3]

1 Department of Vertebrate Zoology, National Museum of Natural History, Smithsonian Institution, Washington, DC, USA
2 Ecological Modelling Services Pty Ltd, University of Queensland, St Lucia, Qld, Australia
3 NOAA, National Marine Fisheries Service, Pacific Islands Fisheries Science Center, Honolulu Laboratory, Honolulu, HI, USA

Keywords
Age; Cheloniidae, *Lepidochelys olivacea*; growth; humeral skeletal anatomy; non-parametric smoothing; North Pacific Ocean; Reptilia; seaturtle growth modeling; skeletochronology; Testudines.

Correspondence
George Zug, PO Box 37012, Amphibian and Reptiles/mrc 162, Smithsonian Institution – NMNH, Washington, DC, USA 20013-7012
E-mail: zugg@si.edu

Accepted: 9 August 2006

doi:10.1111/j.1439-0485.2006.00109.x

Abstract

The olive ridley is the most abundant seaturtle species in the world but little is known of the demography of this species. We used skeletochronological data on humerus diameter growth changes to estimate the age of North Pacific olive ridley seaturtles caught incidentally by pelagic longline fisheries operating near Hawaii and from dead turtles washed ashore on the main Hawaiian Islands. Two age estimation methods [ranking, correction factor (CF)] were used and yielded age estimates ranging from 5 to 38 and 7 to 24 years, respectively. Rank age-estimates are highly correlated ($r = 0.93$) with straight carapace length (SCL), CF age estimates are not ($r = 0.62$). We consider the CF age-estimates as biologically more plausible because of the disassociation of age and size. Using the CF age-estimates, we then estimate the median age at sexual maturity to be around 13 years old (mean carapace size *c.* 60 cm SCL) and found that somatic growth was negligible by 15 years of age. The expected age-specific growth rate function derived using numerical differentiation suggests at least one juvenile growth spurt at about 10–12 years of age when maximum age-specific growth rates, *c.* 5 cm SCL year^{-1}, are apparent.

Problem

Cheloniid seaturtles are long-lived vertebrates, maturing in their early teens or much later and potentially able to reproduce for several decades thereafter. During the past two decades, seaturtle biologists have obtained age estimates for different populations of green, loggerhead, and Kemp's ridley seaturtles (Heppell *et al.* 2003). Not unexpectedly, different populations of the same species and different species have different growth rates and attain sexual maturity at different ages (Bjorndal 2003; Heppell *et al.* 2003; Balazs & Chaloupka 2004; Chaloupka *et al.* 2004). Among these three species, Kemp's ridleys have the smallest adult size [56–78 cm straight carapace length (SCL); Márquez 1994] and the youngest age at sexual maturity (11–16 years; Zug *et al.* 1997). Loggerhead and green seaturtles are significantly larger than ridleys as adults and attain sexual maturity much later, ≥30 years for loggerheads (Chaloupka 2003) and >25 years for greens (Zug *et al.* 2001; Balazs & Chaloupka 2004; Chaloupka *et al.* 2004). In contrast to Kemp's ridleys, olive ridleys occur widely throughout the tropical seas and are the most abundant seaturtle species (Reichart 1993); however, the range of adult size is nearly identical for the two species (53–79 cm SCL – *Lepidochelys olivacea*; Reichart 1993 & Zug *et al.* 1998).

Although Kemp's ridleys are geographically restricted to the western Atlantic basin and the Gulf of Mexico, the olive ridley occurs widely throughout tropical seas and is considered the most abundant seaturtle species. Despite the disparity in distribution, adult size is nearly identical for the two species. Their comparable body sizes and

close phylogenetic affinities (Bowen & Karl 1996) suggest that *L. olivacea* likely shares a similar growth rate and first age at sexual maturity with *L. kempii*. Age data, however, have not been forthcoming for the olive ridley because researchers rarely encounter immature turtles and, hence, have had few opportunities to study young olive ridleys. Instead, research has focused on behavior and ecology associated with annual reproduction activities at nesting beaches (*e.g.* Plotkin *et al.* 1997). The absence of young turtles in coastal waters and near-shore or estuarine 'developmental' habitats suggests that *L. olivacea* juveniles occupy an oceanic habitat (Bolten 2003). Because of the importance of growth and age at first reproduction for population modeling and conservation management of this species, the NOAA/NMFS Pacific Islands Fisheries Science Center in Hawaii slowly accumulated a sample of pelagic olive ridleys for skeletochronological examination. Although the present sample is still small, the number of specimens is now adequate for a preliminary analysis. Importantly for the first time, the sample's range of body sizes offers an opportunity to examine the growth of this species and provide an estimate of age for different sized individuals.

Material and Methods

Data set and morphometric measurements

The data set used here comprised 27 size-at-age records for *Lepidochelys olivacea* – 26 records from salvaged individual turtles plus the inclusion of known mean hatchling size for this species. The data set contains growth records spanning the post-natal development phase (4 cm to approximately 65 cm SCL) to mature adults, although the records are not distributed evenly over this size range. Age estimates were derived from a skeletochronological analysis of 26 olive ridleys salvaged (from 1993 through 2002) from the by-catch capture of the long-line fishery in the vicinity of Hawaii and from coastal strandings in the Hawaiian islands. All individuals were measured to the nearest 0.1 cm SCL. The salvaged turtles ranged from 20.5 to 64.4 cm SCL. Each of the 26 turtles was assigned a maturity score (immature, adult) based on size, gonadal development, and other morphometric considerations. Each turtle was necropsied (see Work & Balazs 2002) and its right humerus removed for skeletochronological examination. The necropsy data included a complete set of carapace measurements, organ condition evaluations, and sex and state of maturity. In the laboratory prior to sectioning of the humeri for histological examination, we recorded 12 morphometric measurements. For this analysis, we use five of these measurements: Maximum length (MaxL), distance from proximal most tip of the ulnar process to distalmost articular surface; Longitudinal length (LongL), distance from proximal surface of humeral head to distalmost articular surface; Proximal length (ProxL), distance from proximal surface of humeral head to distalmost edge of deltopectoral crest; Medial width (MedW), width of humerus (anterior to posterior surface) at the narrowest width of the diaphysis; Thickness (Thick), width of humerus (dorsal to ventral surface) at the narrowest width of the diaphysis. All measurements are straightline distances parallel or perpendicular to the longitudinal axis and recorded to 0.1 mm with dial calipers. These measurements permit an examination of the association of body size (carapace) to humerus size in order to assess the effect of the latter on our estimations of age.

Our skeletochronological data were derived from cross-sections (0.5- to 0.8-mm thick) from the middle of the humeral shaft just distal to the deltopectoral crest and at the narrowest diameter of the diaphysis (Zug *et al.* 1986), because the humerus retains the greatest number of periosteal growth layers there. Hence, this location permits the most accurate estimation of the number of growth cycles (periosteal layers) and the relative rates of growth (= successive humerus diameters). On each specimen, we counted the number of visible growth layers and measured the widths (long-axis diameters) of the humerus at each successive growth cycle and the width of the resorption core using the calibrated metric stage of a compound microscope. Bone sections were not stained and were examined by transmitted light.

Age estimation protocols

Growth and age data can be estimated/extracted from the preceding data set in several ways. We use two age-estimation protocols: (i) ranking (Zug 1990) and (ii) correction factor (CF) (Parham & Zug 1998). The use of two protocols provides a broader perspective of the potential variation in age and growth rates. Both protocols rest on the basic assumption that each successive growth layer represents 1 year in the life of an olive ridley seaturtle. There is no known-aged *L. olivacea* in our sample or from other *L. olivacea* studies to test this assumption. The ranking protocol uses three data items (resorption core diameter, the set of sequential diameters of the complete growth layers, external diameter of humerus at death) to obtain an age estimate of each individual. The first step is to order individuals by the increasing diameters of their individual resorption cores. The rows created by this ordering consist of sequential growth layer diameters from smallest complete layer to the outside diameter. These sequential diameters yield columns of successive increasing diameters, and the innermost diameter for each turtle is assigned to the column to which its diameter most closely match those diameters of preceding turtles.

The assignment of innermost diameter fixes the sequential assignment of column position of all succeeding diameters; no column is skipped in the sequence of diameters. This ranking protocol yields a table with a stepwise appearance because of the increasing size of the innermost diameter of successive individuals. Each column represents 1 year, and the position of the outer diameter denotes the age at death of an individual (Table 1).

In the CF protocol, an estimate of a turtle's age derives from the number of growth layers (= diameters) observed in the outer region of the humerus section plus an estimate of the number of growth layers lost by resorption as the center of humerus is remodeled. The latter, unobservable component is estimated as $(D - D_H)/CF$, where D is the diameter of the resorption core, D_H is the diameter of a hatchling's humerus (before the beginning of increment formation), and CF is the correction factor. The correction factor is a constant 'ageing rate' (year mm^{-1}) assumed to apply to the resorption core and calculated as the mean slope of the successive humeri-growth diameters in a sample of the smaller individual turtles. The *L. olivacea* sample for CF calculation consisted of nine individuals (20.5–55.3 cm SCL) with MedW of 11.9–20.5 mm; the maximum diameter of the subsample encompasses the resorption core diameters of all but four individuals, which have resorption diameters of 22.1–24.8 mm, in the total sample. The least-squares linear regressions of the subsample yielded a mean slope of 2.20 (1.750–2.518, $s = 0.295$), and the regressions were strongly linear ($r = 0.982$–0.999). Thus, CF = 2.20. The mid-diaphyseal diameter of the hatchling *L. olivacea* humerus is 0.8 mm. We use 4.0 cm SCL as an average carapace length for hatchling Pacific ridleys (Márquez *et al.* 1976).

Table 1. Age estimation for ranking and correction factor protocols.

	age estimate (years)	
size (SCL, cm)	ranking protocol	correction factor protocol (CF)
20.5	5	7.3
33.0	12	9.4
38.2	18	12.0
43.7	18	17.0
46.6	24	13.6
47.9	23	13.1
52.7	26	16.7
54.0	27	16.9
55.3	27	16.9
56.5	28	17.9
57.5	34	17.7
57.7	34	18.1
57.7	34	18.6
57.8	33	19.6
60.0	36	24.1
60.2	34	15.7
60.3	37	18.0
60.4	32	23.4
61.6	33	14.8
61.8	31	16.3
62.1	32	13.7
62.1	34	18.1
62.4	37	14.7
62.5	38	12.8
63.0	34	19.3
64.4	38	12.9

SCL, straight carapace length.

Age-specific growth function estimation

We estimated the underlying age-specific growth function using a generalized smoothing spline regression approach implemented in the gss library (Gu 2002), which is available for the statistical modeling program R (Ihaka & Gentleman 1996). Smoothing spline regression uses the data to determine the underlying linear or nonlinear trend without assuming any specific functional form. Confidence or credible bands are derived using Bayesian cross-validation (Gu 2002). We then estimated the age-specific growth rate function by numerically differentiating the expected size-at-age function (Chaloupka *et al.* 2004). We then estimated the underlying age-specific maturity function using a generalized smoothing spline logistic regression approach (Gu 2002).

Results

Gross skeletal anatomy

The humerus of seaturtles is unique among living turtles by the proximal elongation of the ulnar process and reduction of the radial process to a low, but distinct, diagonally transverse ridge distal to the humeral head (Zug 2001; Wyneken 2003). This atypical testudine morphology presumably resulted from the re-positioning of muscle attachments as an adaptation to increase the power and efficiency of the figure-8 forelimb stroke for aqueous flight (Wyneken 1996).

This morphology is evident in hatchling seaturtles. Differential growth in some humeral segments during early juvenile development amplifies the unique morphology; however, the extent of differential growth in the earliest stages cannot be documented with our data, because of the absence of small turtles in our sample. Nonetheless, it remains evident in our sample of older/larger individuals by differences in linear-regression slopes. These allometric relationships are strongly linear. The least squares linear regression and correlation coefficients are: MaxL = −11.474 + 2.442 SCL, $r = 0.97$, $P < 0.001$; LongL =

−7.310 + 2.224 SCL, $r = 0.98$, $P < 0.001$; ProxL = −0.930 + 0.795 SCL, $r = 0.96$, $P < 0.001$; MedW = 3.234 + 0.317 SCL, $r = 0.94$, $P < 0.001$; Thick = −0.100 + 0.196 SCL, $r = 0.93$, $P < 0.001$; Thick = −1.485 + 0.588 MedW, $r = 0.94$, $P < 0.001$. Visual comparison of scatterplots confirms the linearity and absence of any outliers for the sample (n = 26). The MedW is recorded from the humerus prior to the removal of two cross-sections for microscopic examination. The maximum width or diameter (OutsideD) of a section is recorded simultaneously with data for the sequential growth-layer diameters. Ideally, OutsideD and MedW are equal; however, the section-examined is unlikely to derive from the same position as the MedW measurement. Our data set has only one specimen in which the OutsideD value is less than MedW; although the differences between pairs of values is slight, the distribution functions of the row samples are significantly different (Wilcoxon sign ranks test, $Z = 3.799$, $P < 0.005$). A linear regression reveals the high similarity of the individual values ($r = 0.96$, $P < 0.001$, MedW = 2.866 + 0.827 OutsideD). OutsideD is also highly correlated ($r = 0.94$, $P < 0.001$) with SCL (OutsideD = 0.332 + 0.385 SCL). This latter association is important for the subsequent estimate of growth-rates from back-calculated SCLs of each individual using the sequential growth-layer diameters.

Microscopic skeletal anatomy

From the restricted perspective of the middle of the diaphysis, bone organization in the olive ridley humerus matches the general pattern observed in other cheloniid turtles. In outline, the mid-diaphysis is oblong on the anterior–posterior axis. The periphery consists of compact bone, and the center, about two-thirds the area of the cross-section, is cancellous (spongy) bone (Fig. 1 top). This cancellous core is a site of active resorption and redeposition of bone and is a constantly enlarging area. The peripheral compact bone shows the layering resulting from the cycling of periosteal growth. These layers are the essential ingredients of skeletochronology, providing the record of the individual's cyclic growth pattern. Viewed through transmitted light, each layer consists of a broad band of lightly colored bone and a narrower band of dark bone (Fig. 1 left), representing, respectively, periods of rapid and slower growth. Lines of arrested growth (LAGs) are not evident with transmitted light; however, polarized light reveals the difference in the density of bone struc-

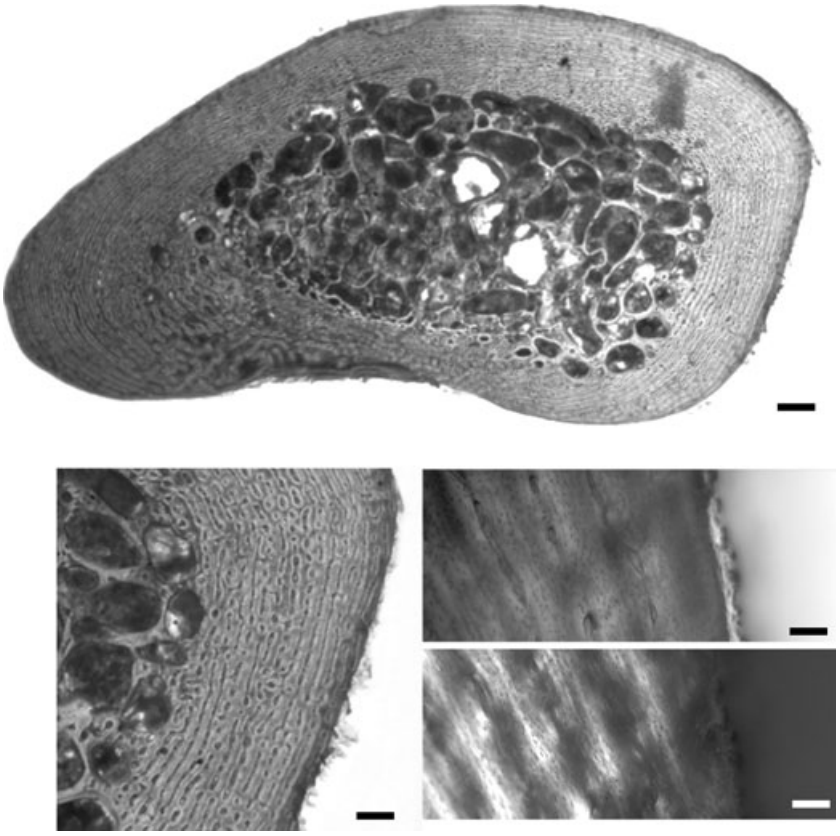

Fig. 1. Top: Cross-section of a *Lepidochelys olivacea* humerus at mid-diaphysis, transmitted light of unstained section. Bottom left: Magnified view of the right side of the total section above it; dusky areas between vascularized bands contain the zones of slow and no growth. Bottom right: Magnified section (100X) of growth layers viewed under transmitted (top) and polarized (bottom) light; bright lines denote Lines of arrested growths. Scale bars: top: 1 mm, bottom left: 0.5 mm, middle and bottom right: 0.12 mm.

ture produced as growth slows and stops, *i.e.* LAGs are present (Fig. 1 bottom right) within each dark zone as the bright lines.

Our measurements of successive growth layers yielded a series of mid-diaphyseal diameters of the humeri, *i.e.* a diameter for each successive season of growth. These diameters can be used to estimate the sequential increase in body size (SCL) because of the high linear correlation between the diameter of the humerus and the carapace. In other cheloniid seaturtles (*e.g.* Zug *et al.* 2001), the pattern of diameter growth has been predominantly a pattern of decreasing diaphyseal diameters and growth-layer widths (thickness) within each individual. This is not the pattern for *L. olivacea*. There is both a high level of uniformity in amount of growth within each individual and among all individuals. The differences in layer thickness (width) between successive diameters (delta-growth, D_g) illustrates this homogeneity (Fig. 2). Twenty individuals in our sample yielded 122 D_gs; the D_gs range between 0.05 and 0.60 mm with mean of 0.229 (s = 0.072) and median of 0.25 mm for the total sample. Examined individually, nine turtles had medians of 0.20 and six with 0.25 mm medians (75% of total sample). An ANOVA showed no significant difference among the means of 20 individuals ($F = 0.97$, df 19, $P = 0.50$). Six of the 12 largest (SCL ≥ 60 cm) turtles did not display LAG on one side of the humerus section; hence layer widths could not be determined for them. Four of these were healthy individuals caught on longlines.

Skeletochronology

The preceding D_gs and successive growth layer (humeral) diameters are the data necessary for estimating the ages of the seaturtles. As demonstrated above in the gross anatomical section, there are strong, positive relationships among the longitudinal and transverse measurements of the humerus and carapace length. In contrast, neither humerus dimensions nor carapace length is associated with growth layer widths [*e.g.* $r = 0.132$ ($P = 0.603$) and 0.005 ($P = 0.985$), mean layer width to MaxL and SCL, respectively].

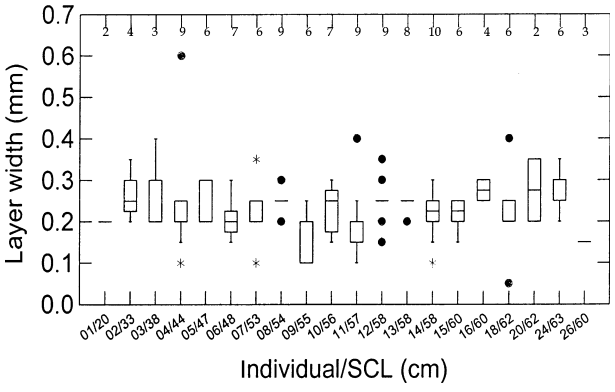

Fig. 2. Box plots of growth layer thicknesses for each turtle of our skeletochronological sample with two or more complete growth layers. Thickness equals the difference between successive diameters divided by two. Horizontal line, median; box, limits of second and third quartiles; vertical line, range; asterisk, outlier; dot, distant outlier. Sample sizes for each individual are along the top horizontal.

Of the 26 individuals examined, we were able to obtain age-estimates for all individuals. The CF age estimates range from 7.3 to 24.1 years, and the ranking protocol yields 5–38 years (Table 1). In both estimate protocols, the smallest turtle in the sample has the lowest age estimate. CF and Ranking age estimates are similar only in the smallest turtles (*i.e.* 20–44 cm SCL); thereafter, the differences between the two increase with maximum differences occurring in the largest turtles, those >60 cm SCL. With the exception of the smallest turtle, the Ranking age estimates are higher (older) for all individuals. This difference is most apparent in age estimates for the 62.5- and 64.4-cm SCL olive ridleys with 38 years (Ranking) and 13 years (rounded CF) for both turtles. This comparison illustrates that CF estimates are uncoupled from the size of a turtle, whereas Ranking estimates are not. It is this coupling to size that results in a stronger linear relationship between age and size in the Ranking estimates ($r = 0.93$, $P < 0.001$) *versus* the CF ones ($r = 0.62$, $P = 0.001$). The uncoupling of size and age is also evident because the oldest CF-aged turtles (both 60 cm SCL) are not the largest turtles.

Using the minimum SCL (53 cm) for nesting females as a determinant of sexual maturity, CF estimates yield 13 years or less (youngest age estimate is the largest ridley) and 26 years (Rank) for the 52.7 cm ridley. The six turtles <53 cm SCL range in estimated age from 7 to 17 years (CF) and 5 to 23 years (Rank). We consider the CF age estimates as biologically more plausible because of the disassociation of age and size, and we use these age-estimates in all subsequent analyses.

Age-specific growth functions

The expected age-specific growth function for the CF age estimates is shown in Fig. 3a. The function is not well estimated for ages ranging from hatching to about 6 years of age due to the limited data, which is indicated by the wide credible bands. Somatic growth appears to plateau at about 15 years of age. The expected age-specific logistic maturity function based on the CF age estimates is shown in Fig. 3b. The function shows that 50% maturity is estimated to occur at around 13 years of age but there is significant uncertainty around the estimate function as indicated by the very wide upper bound for age estimates <10 years of age.

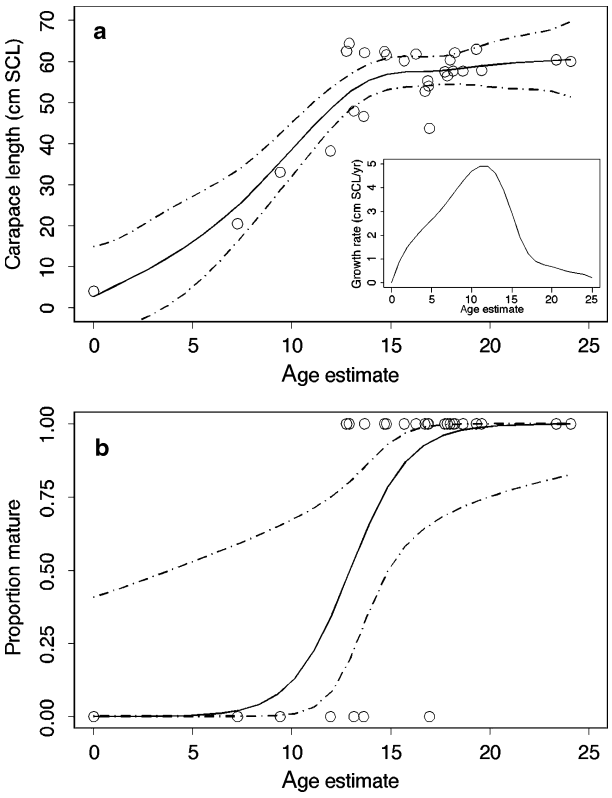

Fig. 3. Panel (a) shows the expected size-at-age growth function (solid curve) fitted using a generalized smoothing spline model (Gu 2002) with 95% credible interval shown by the dashed curves. Age estimates shown by open dots and an estimate for expected olive ridley hatchling size is also included. Inset shows the age-specific growth rate function derived by numerical differentiation of the expected size-at-age function [solid curve in panel (a)]. Panel (b) shows the expected age-specific maturity function (solid curve) also fitted using a generalized smoothing spline model with 95% credible interval shown by the dashed curves, and open dots show the individual binary response variable (immature, mature).

Discussion

The olive ridley seaturtle is the most abundant sea turtle species in the world but little is known of the demography of this species (Reichart 1993). We used skeletochronological techniques to derive the first estimates of age and age-specific growth functions for the olive ridley, which are essential for understanding the population dynamics of this species (Chaloupka & Musick 1997).

Gross skeletal anatomy

All measurements, parallel or perpendicular to longitudinal axis, of the humerus are strongly correlated ($r \geq 0.93$) with carapace length (SCL). Different linear regression slopes denote allometric growth. For example, the slope of MaxL and LongL are nearly equivalent (2.44 and 2.22, respectively) and differ strikingly from that of ProxL (0.80). These values indicate that the overall length of the olive ridley humerus increases relatively rapidly and the ulnar process increases faster than the main diaphyseal shaft, *i.e.* MaxL and LongL includes the ulnar process as part of the measurement, ProxL does not. In contrast, the radial process-deltopectoral crest segment grows at a rate slower than the overall lengthening of the humerus. Comparison of MedW and Thick slopes indicates the diaphysis broadens somewhat faster in the anteroposterior axis than in the dorsoventral one.

No one has closely examined the allometry within seaturtle fore- or hindlimbs although evidence exists for differences in flipper (forelimb) morphology with cheloniid seaturtles. Wyneken *et al.* (1999) showed differences in size and shape of flippers between Atlantic and Pacific juvenile *Chelonia mydas*. Our data highlight possible trends in limb morphology and the potential of these growth trends to reveal differences in locomotor patterns and performance among different life stages of the same species and among different populations and species. They do not, however, allow more detailed analysis.

Microscopic skeletal anatomy

The general appearance of the *L. olivacea* humeral sections (Fig. 1 top) does not differ from that in other seaturtles (Bjorndal *et al.* 2003: Fig. 2). Unstained bone examined with transmitted light often does not show sharply defined LAGs, rather large dusky zones of slow growth. The regular widths of the bony growth layers, however, are not a common phenomenon, and we have not observed them previously in cheloniid seaturtles. The typical pattern is one of declining layer width (thickness) with the increasing size of the turtle. The regularity in olive ridleys suggest a more pulsed and regulated growth of the limb skeleton, observed in the humerus and presumably also occurring in the antebrachial and hindlimb elements. The revelation of LAGs by polarized light (Fig. 1 bottom right) convinced us that bone growth in *L. olivacea* shares an annual pattern as in *Caretta caretta* (Klinger & Musick 1992; Coles *et al.* 2001; Bjorndal *et al.* 2003) and *L. kempii* (Snover & Hohn 2004). The LAGs and the annual growth pattern of *C. mydas* in the relatively constant-temperature water of the Hawaiian area (Zug *et al.* 2001) indicated that seaturtle bone-growth responds to some external or internal stimulus other than or in addition to fluctuation of water temperatures. None of our data addresses either the cyclic nature or uniformity of growth in *L. olivacea*.

Skeletochronology: age estimates

The two age-estimate protocols yield strikingly different estimates: 7–24 and 5–38 years for CF and Ranking, respectively. Because the Ranking estimates are highly correlated to SCL as well as greater than those for the congeneric Kemp's ridley, we accept the CF estimates as the biologically more plausible ones.

The age-specific growth function (Fig. 3a) shows that the somatic growth rate slows and begins to plateau at about 15 years (see also the age-specific growth rate function in the inset). The age-specific logistic maturity function shows 50% maturity around 13 years; however, there is significant uncertainty around this estimated function as indicated by the very high upper boundary of the confidence limits for age estimates <10 years.

The phenomenon of some individuals growing slower and maturing later is not an uncommon aspect of turtle biology (Congdon *et al.* 2003) and can result from an individual being the 'runt of a litter' or suffering an injury or disease that slows its growth. The general pattern of *L. olivacea* growth appears slower than that of *L. kempii* (see Chaloupka & Zug 1998: Fig. 1). Based on CF ages, *L. olivacea* is around 35–40 cm SCL at 10-year old; however, some 60+ cm SCL individuals have age-estimates of 13–14 years. The discrepancy between these two observations emphasizes the limited nature of our sample for individuals <50 cm SCL. This limitation also does not permit us to discern the presence or absence of polyphasic growth (Chaloupka & Zug 1998) in *L. olivacea*, which has been re-confirmed for *L. kempii* of the eastern Gulf of Mexico (Schmid & Barichivich 2005).

Excluding the six ridleys with SCL >60 cm and CF age-estimates <16 years yields a growth curve that suggests an even slower growth pattern for the olive ridley. Additional manipulations of the age and size observations promote other speculations due to limited data. Rather than speculate, the presence of large, young turtles suggests a broad age-range for the attainment of sexual maturity. These large, young turtles indicate that maturity might occur as early as 10 years. On the other hand, the smaller, older individual suggests a later maturity of 15–18 years. Such a broad range does not conflict with chelonian reproductive biology, nor specifically with reproductive data of the congeneric Kemp's ridley. In the latter, head-start turtles provide known-aged individuals, and records of their first nesting gives a range of 10–18 years (Shaver 2005).

Skeletochronology: growth estimates

We present the first age and age-specific growth functions for the olive ridley seaturtle (Fig. 3). Schmid & Barichivich (2005) provided a set of size-specific growth rate estimates for Kemp's ridleys from the eastern Gulf of Mexico. These rates were based on recapture measurements and yield a mean growth rate of *c.* 4.2 cm SCL per year (recalculated from their Table 2). Chaloupka & Zug (1998) estimated a polyphasic age-specific growth rate function for the Kemp's ridley and found age-specific growth rates of *c.* 5–6 cm SCL per year for this species in the second growth phase around 8 years of age. We found growth rates of *c.* 5 cm SCL per year for the olive ridley around 10–12 years of age (see inset in Fig. 3a). So it is possible that the widely distributed olive ridley seaturtle and the endemic Kemp's ridley seaturtle have similar growth patterns and characteristics. In spite of our initial hesitancy to attribute the regularity of the humerus's circumferential growth to an annual cycle, *i.e.* one layer equals 1 year of growth, the preceding analyses of the skeletochronological data reveal aging and growth patterns of *L. olivacea* that match those of its congener *L. kempii* and fit the overall cheloniid patterns when adjusted for this species' smaller size at sexual maturity.

Acknowledgements

The following individuals and organizations have contributed to this research project: G. Antonelis, C. Hooven, R. Morris, S.K.K. Murakawa, T. Work, the State of Hawaii Department of Land and Natural Resources, the Hawaii Preparatory Academy, and the Marine Option Program of the University of Hawaii (Manoa and Hilo). G. Zug thanks the NOAA-NMFS Pacific Islands Fisheries Science Center for encouraging and supporting our research in seaturtle biology. G. Zug also acknowledges the long-term support of the SI/NMNH Department of Vertebrate Zoology for his skeletochronological research. We thank B. Bowen, A. Hohn, and M. Snover for their advice, which improved the clarity of this report.

References

Balazs G., Chaloupka M. (2004) Spatial and temporal variability in somatic growth of green sea turtles resident within the Hawaiian Archipelago. *Marine Biology*, **145**, 1043–1059.

Bjorndal K.A. (2003) Roles of loggerhead sea turtles in marine ecosystems. In: Bolten A.B., Witherington B.E. (Eds), *Loggerhead Sea Turtles*. Smithsonian Books, Washington: 235–254.

Bjorndal K.A., Bolten A.B., Dellinger T., Delgardo C., Martins H.R. (2003) Compensatory growth in oceanic loggerhead sea turtles: response to a stochastic environment. *Ecology*, **84**, 1237–1249.

Bolten A. (2003) Variation in sea turtle life history patterns, neritic *versus* oceanic developmental stages. In: Lutz P., Musick J., Wyneken J. (Eds), *The Biology of Sea Turtles*.

CRC Marine Science Series, CRC Press, Boca Raton, Florida: 243–257.

Bowen B.W., Karl S.A. (1996) Population genetics phylogeography, and molecular evolution. In: Lutz P.L., Musick J.A. (Eds), *The Biology of Sea Turtles*. CRC Press, Boca Raton, Florida: 29–50.

Chaloupka M. (2003) Stochastic simulation modelling of loggerhead sea turtle population dynamics given exposure to competing mortality risks in the western south Pacific. In: Bolten A.B., Witherington B. (Eds), *Loggerhead Sea Turtles*. Smithsonian Press, Washington, DC: 274–294.

Chaloupka M., Musick J.A. (1997) Age, growth and population dynamics. In: Lutz P., Musick J. (Eds), *The Biology of Sea Turtles*. CRC Marine Science Series, CRC Press, Boca Raton, Florida: 233–276.

Chaloupka M., Zug G.R. (1998) A polyphasic growth function for the endangered Kemp's ridley sea turtle, *Lepidochelys kempii*. *Fishery Bulletin*, **95**, 849–856.

Chaloupka M., Limpus C.J., Miller J. (2004) Green turtle somatic growth dynamics in a spatially disjunct Great Barrier Reef metapopulation. *Coral Reefs*, **23**, 325–335.

Coles W.C., Musick J.A, Williamson L.A. (2001) Skeletochronology validation from an adult loggerhead (*Caretta caretta*). *Copeia*, **2001**, 240–242.

Congdon J.D., Nagle R.D., Kinney O.M., van Loben Sels R.C., Quinter T., Tinkle D.W. (2003) Testing hypotheses of aging in long-lived painted turtles (*Chrysemys picta*). *Experimental Gerontology*, **38**, 765–772.

Gu C. (2002) *Smoothing Spline ANOVA Models*. Springer-Verlag, New York, New York.

Heppell S.S., Snover M.L., Crowder L.B. (2003) Sea turtle population ecology. In: Lutz P., Musick J., Wyneken J. (Eds), *The Biology of Sea Turtles*. CRC Marine Science Series, CRC Press, Boca Raton, Florida: 275–306.

Ihaka R., Gentleman, R. (1996) R: a language for data analysis and graphics. *Journal of Computations, Graphics and Statistics*, **5**, 299–314.

Klinger R.-E.C., Musick J.A. (1992) Annular growth layers in juvenile loggerhead turtles (*Caretta caretta*). *Bulletin of Marine Science*, **51**, 224–230.

Márquez R. (1994) Synopsis of biological data on the Kemp's ridley turtle, *Lepidochelys kempi* [sic] (Garman, 1880). *NOAA Technical Memorandum*, NMFS-SEFSC-343, 1–91.

Márquez R., Villanueva -O.A., Peñaflores -S.C. (1976) Sinopsis de datos biologicos sobre la tortuga golfina *Lepidochelys olivacea* (Eschscholtz, 1892). *INP Sinopsis sobre la Pesca*, **2**, 1–61.

Parham J.F., Zug G.R. (1998) Age and growth of loggerhead sea turtles (*Caretta caretta*) of coastal Georgia: an assessment of skeletochronological age-estimates. *Bulletin of Marine Science [1997]*, **61**, 287–304.

Plotkin P.T., Rostal DC., Byles R., Owens D.W. (1997) Reproductive and developmental synchrony in female *Lepidochelys olivacea*. *Journal of Herpetology*, **31**, 17–22.

Reichart H.A. (1993) Synopsis of biological data on the olive ridley sea turtle *Lepidochelys olivacea* (Eschscholtz, 1829) in the western Atlantic. *NOAA Technical. Memorandum*, NMFS-SEFSC-336, 1–78.

Schmid J.R., Barichivich W.J. (2005) Developmental biology and ecology of the Kemp's ridley sea turtle, *Lepidochelys kempii*, in the eastern Gulf of Mexico. *Chelonian Conservation and Biology*, **4**, 828–834.

Shaver D.J. (2005) Analysis of the Kemp's ridley imprinting and headstart project at Padre Island National Seashore, Texas, 1978–88, with subsequent nesting and stranding records on the Texas coast. *Chelonian Conservation and Biology*, **4**, 846–859.

Snover M.L., Hohn A.A. (2004) Validation and interpretation of annual skeletal marks in loggerhead (*Caretta caretta*) and Kemp's ridley (*Lepidochelys kempii*) sea turtles. *Fishery Bulletin*, **102**, 682–692.

Work T.M., Balazs G.H. (2002) Necropsy findings in sea turtles taken as bycatch in the North Pacific longline fishery. *Fishery Bulletin*, **100**, 876–880.

Wyneken J. (1996) Sea turtle locomotion: mechanisms, behavior, and energetics. In: Lutz P.L., Musick J.A. (Eds), *The Biology of Sea Turtles*. CRC Press, Boca Raton, Florida: 165–198.

Wyneken J. (2003) The external morphology, musculoskeletal system, and neuro-anatomy of sea turtles. In: Lutz P., Musick J., Wyneken J. (Eds), *The Biology of Sea Turtles*. CRC Marine Science Series, CRC Press, Boca Raton, Florida: 39–77.

Wyneken J., Balazs G.H., Murakawa S.K.K., Anderson Y. (1999) Size differences in the hind limbs and carapaces of hatchling green turtles (*Chelonia mydas*) from Hawaii and Florida, USA. *Chelonian Conservation and Biology*, **3**, 491–495.

Zug G.R. (1990) Age determination of long-lived reptiles: some techniques for seaturtles. *Annales des Sciences Naturelles, Zoologie*, **11**, 219–222.

Zug G.R. (2001) Turtles of the Lee Creek Mine (Pliocene). *Smithsonian Contributions to Paleobiology*, **90**, 203–218.

Zug, G.R., Wynn A.H., Ruckdeschel, C. (1986) Age determination of loggerhead sea turtles, *Caretta caretta*, by incremental growth marks in the skeleton. *Smithsonian Contributions to Zoology*, **427**, 1–34.

Zug G.R., Kalb H.J., Luzar S.J. (1997) Age and growth in wild Kemp's ridley seaturtles *Lepidochelys kempii* from skeletochronological data. *Biological Conservation*, **80**, 261–268.

Zug G.R., Ernst C.H., Wilson R.V. (1998) *Lepidochelys olivacea* (Eschscholtz) olive ridley seaturtle, tortuga golfina, lora. *Catalogue of American Amphibians and Reptiles*, **653**, 1–13.

Zug G.R., Balazs G.H., Wetherall J.A., Parker D.M., Murakawa S.K.K. (2001) Age and growth of Hawaiian green seaturtles (*Chelonia mydas*): an analysis based on skeletochronology. *Fishery Bulletin*, **100**, 117–127.